



Minerva Access is the Institutional Repository of The University of Melbourne

Author/s:

Weij, R;Woodhead, JD;Sniderman, JMK;Hellstrom, JC;Reed, E;Bourne, S;Drysdale, RN;Pollard, TJ

Title:

Cave opening and fossil accumulation in Naracoorte, Australia, through charcoal and pollen in dated speleothems

Date:

2022-12-01

Citation:

Weij, R., Woodhead, J. D., Sniderman, J. M. K., Hellstrom, J. C., Reed, E., Bourne, S., Drysdale, R. N. & Pollard, T. J. (2022). Cave opening and fossil accumulation in Naracoorte, Australia, through charcoal and pollen in dated speleothems. *Communications Earth and Environment*, 3 (1), <https://doi.org/10.1038/s43247-022-00538-y>.







Persistent Link:

<https://hdl.handle.net/11343/318350>


License:

[CC BY](#)

## Cave opening and fossil accumulation in Naracoorte, Australia, through charcoal and pollen in dated speleothems

Rieneke Weij <sup>1,6</sup>, Jon D. Woodhead <sup>1</sup>, J. M. Kale Sniderman <sup>1</sup>, John C. Hellstrom <sup>1</sup>, Elizabeth Reed<sup>2,3</sup>, Steven Bourne<sup>4</sup>, Russell N. Drysdale <sup>1,5</sup> & Timothy J. Pollard<sup>1,5</sup>

Caves are important fossil repositories which provide records extending back over million-year timescales. While the physical processes of cave formation are well understood, the timing of initial cave development and opening—a more important parameter to studies of palaeontology, palaeoanthropology and archaeology—has proved more difficult to constrain. Here we investigate speleothems from the Naracoorte Cave Complex in southern Australia, with a rich record of Pleistocene vertebrate fossils (including extinct megafauna) and partly World Heritage-listed, using U-Th-Pb dating and analyses of their charcoal and pollen content. We find that, although speleothem formation began at least 1.34 million years ago, pollen and charcoal only began to be trapped within growing speleothems from 600,000 years ago. We interpret these two ages to represent the timing of initial cave development and the subsequent opening of the caves to the atmosphere respectively. These findings demonstrate the potential of U-Th-Pb dating combined with charcoal and pollen as proxies to assess the potential upper age limit of vertebrate fossil records found within caves.

<sup>1</sup>School of Geography, Earth and Atmospheric Sciences, University of Melbourne, Melbourne, VIC, Australia. <sup>2</sup>School of Biological Sciences, University of Adelaide, Adelaide, SA, Australia. <sup>3</sup>Earth and Biological Sciences (Palaeontology), South Australian Museum, Adelaide, SA, Australia. <sup>4</sup>Limestone Coast Landscape Board, Mount Gambier, SA, Australia. <sup>5</sup>Environnements, Dynamiques et Territoires de la Montagne, UMR CNRS, Université de Savoie-Mont, Chambéry, France. <sup>6</sup>Present address: Human Evolution Research Institute/Department of Geological Sciences, University of Cape Town, Cape Town, South Africa. email: [rieneke.weij@uct.ac.za](mailto:rieneke.weij@uct.ac.za)

The provision of robust time constraints on the evolution of cave systems and the sediments that they preserve is crucial to studies of landscape evolution, floral and faunal biodiversity, and human origins. Several different methods (e.g., refs. 1,2) have been applied to this task including palaeomagnetic dating, the use of indicator fossils, and absolute chronometers employing radiometric (e.g., radiocarbon, U-series, or cosmogenic nuclides  $^{26}\text{Al}$ - $^{10}\text{Be}$ ) and luminescence (e.g., thermoluminescence, optically stimulated luminescence (OSL) or infrared stimulated luminescence) techniques. This remains challenging work, however, due to limitations inherent to the dating methods themselves and because in-fill sediments often lag cave development<sup>1</sup>. Speleothems—secondary cave carbonates such as stalagmites and flowstones—have an important role to play here in that they can be precisely and accurately dated using the U-Th and U-Pb chronometers<sup>3,4</sup> across million-year timescales<sup>5</sup>. In this study we develop two novel speleothem proxies for cave ventilation/opening—charcoal and pollen. Sedimentary charcoal is a widely used palaeoenvironmental indicator of biomass burning<sup>6</sup>, but only rarely applied in cave-related studies, primarily to reconstruct human activity<sup>7</sup> or to develop wild-fire histories<sup>8</sup>; it has not been used previously in the context of cave ventilation. Similarly, while the study of fossil pollen is well-established, speleothem palynology is an emerging field<sup>9</sup>. However, since both charcoal and pollen can be transported into caves by wind (and pollen also by animals<sup>10</sup>), their presence within speleothems can provide important information on the timing and extent of cave opening.

To test this premise, we studied the Naracoorte Cave Complex (NCC) (Fig. 1) in southern Australia, a site chosen because of its rich record of Quaternary vertebrate fauna including Australia's extinct megafauna<sup>11</sup>. Previously published ages for the fossil deposits (Fig. 2a and Supplementary Table 1) range from Holocene to Middle Pleistocene (ca. <1–>400 ka)<sup>12–16</sup> with the potential for older deposits based only on speculative ages of ~500 ka<sup>13,17</sup>. However, the absolute antiquity of the NCC and the sediments preserved therein remain highly uncertain because the chronometers previously employed (U-Th, OSL, electron spin resonance) are limited in age range and/or precision.

Previous attempts to unravel the timing of initial cave development focused on dating a fossil dune ridge, the East Naracoorte Range, directly overlying the cave system (Fig. 1c). This ridge is one of the oldest of a series of Pleistocene to Holocene fossil dune ridges (Fig. 1b) that record progressive interglacial sea-level high stands from Naracoorte westward to the modern coastline<sup>18</sup> in response to neotectonic uplift in southern Australia<sup>19</sup>. As the East Naracoorte Range was uplifted along the Kanawinka Fault<sup>20</sup>, it records the last sea-level high stand at Naracoorte, and therefore its age can potentially provide a maximum age for when the system rose above the phreatic zone, i.e., the time of initial cave development. Palaeomagnetic dating<sup>21</sup> shows that the Brunhes-Matuyama reversal lies between the West and East Naracoorte Ranges, suggesting that the latter must be older than 781 ka. Subsequent studies using TL<sup>22–24</sup>, OSL<sup>25,26</sup> and amino-acid racemization (AAR) dating<sup>27</sup> produced maximum ages of

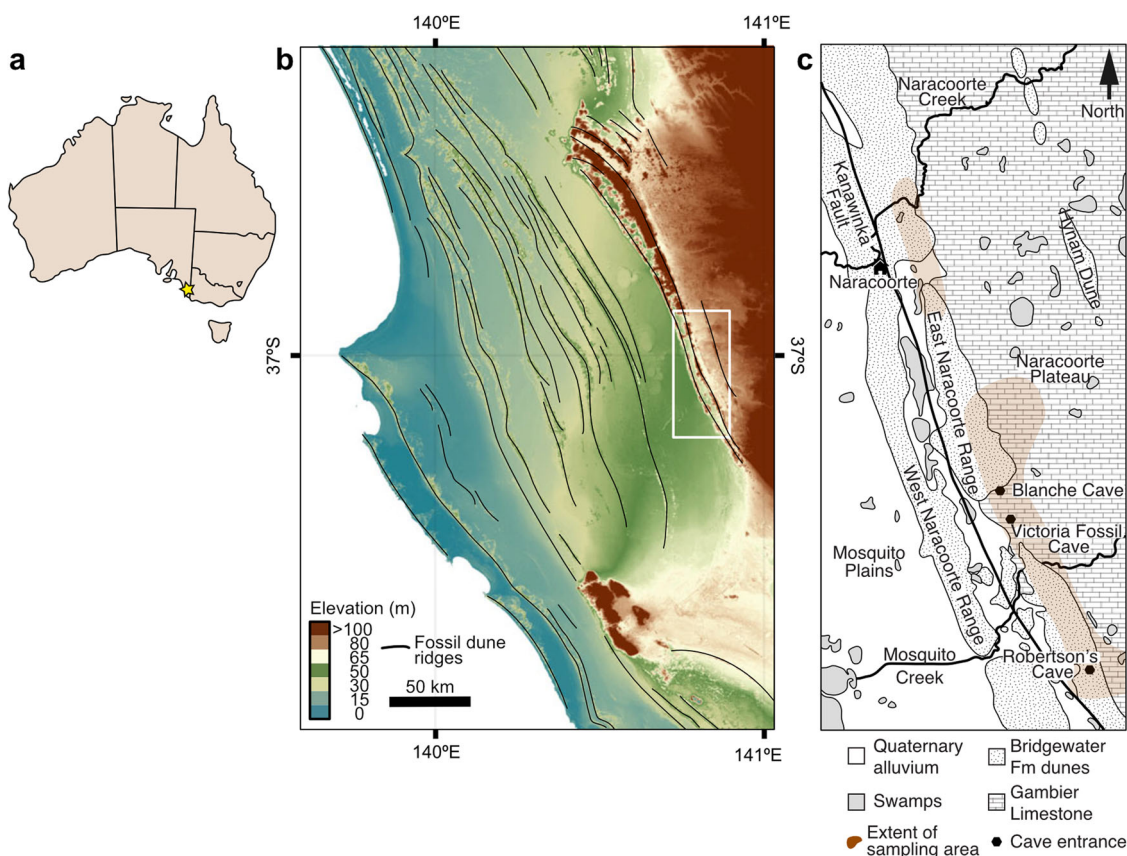


**Fig. 1 Overview and geological map of the Naracoorte Cave Complex (NCC) and analysis of the speleothem ages versus elevation.** **a** Location map showing the study site (yellow star). **b** Shuttle Radar Topography Mission (SRTM) image of coastal southeast South Australia and the NCC (indicated by the white rectangle) with Pleistocene and Holocene fossil dune ridges highlighted by thin black lines, modified after Murray-Wallace<sup>18</sup>. **c** Geological map of the study area modified after White and Webb<sup>20</sup>. The NCC is concentrated along an uplifted portion of the Gambier Limestone, overlain by the Pleistocene East Naracoorte Range. The main tourist caves are depicted by black dots; the rest of the sampling area is indicated simply by a brown shade, as some caves are on private property.

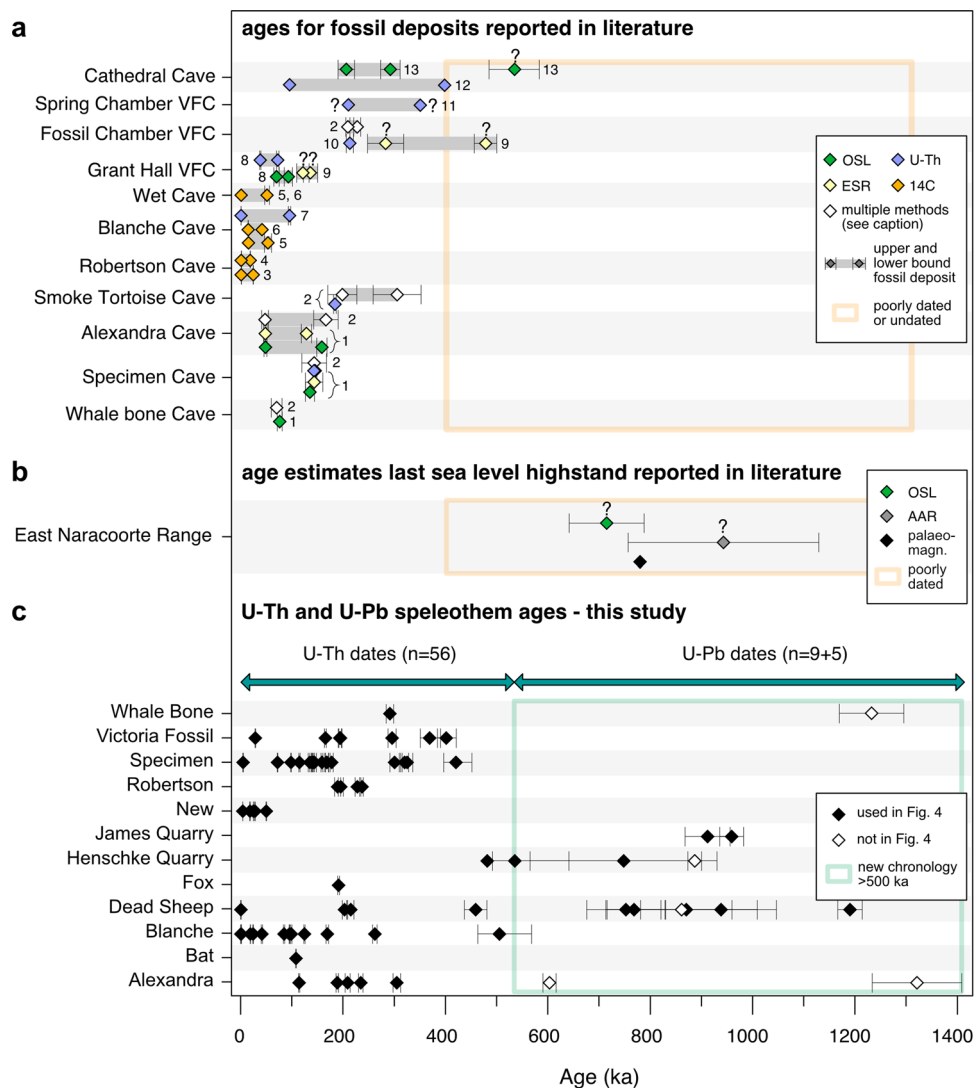


**Fig. 2 Overview of published and new chronological data for the Naracoorte Cave Complex (NCC).** **a** Published ages for the fossil deposits from ten caves within the NCC. VFC Victoria Fossil Cave, 1. Priya et al.<sup>15</sup>, 2. Arnold et al.<sup>16</sup>, 3. Atkins et al.<sup>12</sup>, 4. Grealy et al.<sup>60</sup>, 5. Macken et al.<sup>61</sup>, 6. Darrenougue et al.<sup>62</sup>, 7. St Pierre et al.<sup>63,64</sup>, 8. Macken et al.<sup>65</sup>, 9. Grün et al.<sup>66</sup>, 10. Ayliffe et al.<sup>31</sup>, 11. Moriarty et al.<sup>17</sup>, 12. Brown and Wells<sup>67</sup>, 13. Prideaux et al.<sup>13</sup>. Grey bars show the range between the upper and lower age estimates of each fossil layer. All age uncertainties (whiskers) are reported as 2σ. Note that several age estimates were reported without age uncertainties. **b** Published ages for deposition of the East Naracoorte Range (see text). **c** New U-Th and U-Pb speleothem ages and their 2σ uncertainties (whiskers) from this study. Note that 5 U-Pb ages (open boxes) were not analysed for charcoal and pollen content and are excluded from Fig. 4.

720 ± 70 ka (OSL) and 935 ± 178 ka (AAR), while White and Webb<sup>20</sup> suggested that the caves started to form between 1.1 and 0.8 Ma. However, none of these attempts have proved definitive: the OSL age is far beyond the limit of the technique<sup>28</sup> and AAR is usually best employed together with independent calibration or as a relative dating tool<sup>29</sup>. The age of the East Naracoorte Range, and thus the timing of initial cave development, still remain highly uncertain.

The recent development of the speleothem U-Pb chronometer allows accurate and precise dating of cave deposits far beyond the ~600 ka limit of the U-Th method<sup>30</sup>. Here we first present a new U-Th and U-Pb chronology of the NCC shedding new light on its antiquity. We then integrate charcoal and pollen analyses to provide insight into the timing of cave opening and hence the potential for the discovery of older (>300 ka) fossil deposits. The combination of these novel methodologies has important implications beyond the vertebrate palaeontology community; for example, in studies of archaeology, karst geomorphology and landscape evolution.

**Results and discussion**

**Speleothem U-Th and U-Pb ages.** In combination with new U-Th ages, we present the first U-Pb dates obtained on speleothems from the NCC, extending knowledge of its development prior to 500 ka (Supplementary Table 2). In total we analysed 71 samples for U-Th, of which 15 were within uncertainty of the infinite-age isochron; the latter were then dated with U-Pb techniques (Fig. 3 and Supplementary Fig. 1). The new Naracoorte record spans the Early Pleistocene to Holocene interval, from ~1.3 Ma to ~1.2 ka. The uncertainty on the U-Th ages increases systematically with increasing age, a characteristic inherent to the chronometer. As a result, the age precision (2se) on the younger ages (from 0 ka to ~350 ka) is usually 1–2% with some exceptions resulting in 3% on average, whereas beyond 350 ka uncertainties average 11%. Precision of the U-Pb ages, which depends on the quality of the isochron regression, varied from 1–29% with most samples (n = 13) characterised by a precision better than 11%. Although these uncertainties are

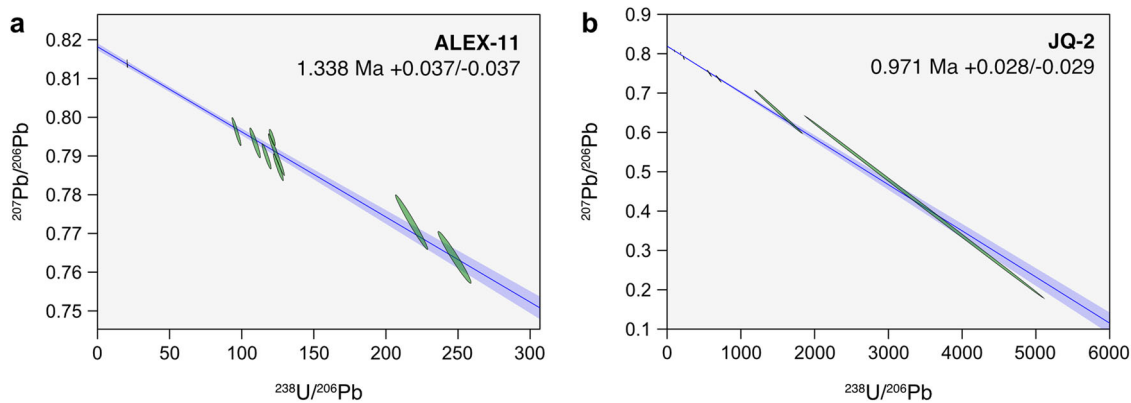


**Fig. 3** Example U-Pb isochrons from two speleothem samples from the Naracoorte Cave Complex. **a** Stalagmite sample ALEX-11 from Alexandra cave. **b** Flowstone sample JQ-2 from James Quarry. See Supplementary Fig. 1 for all U-Pb isochrons.

relatively high for the U-Pb method, due largely to the extremely low U contents encountered (typically ~150 ppb), such uncertainties are an improvement upon results from other dating techniques which have been applied to cave sediments (e.g., OSL, AAR, cosmogenic nuclides). Previously, speleothems from the NCC have only been dated with the U-Th chronometer<sup>17,31</sup>; our new data significantly improve the existing speleothem chronology and extend it by ~70%.

**Improved knowledge of the antiquity of the Naracoorte Cave Complex.** Although previously reported ages for the Naracoorte region remain inconclusive, palaeomagnetic data suggest that cave development may have begun in the Early Pleistocene. The existing speleothem chronology<sup>17,31,32</sup> has been of limited use in this context because the system is clearly beyond the reach of the U-Th chronometer. Among the new U-Pb ages from this study are speleothems that were growing in several caves as early as  $1.34 \pm 0.04$  Ma (stalagmite ALEX-11),  $1.23 \pm 0.08$  Ma (flowstone WB-6) and  $1.20 \pm 0.02$  Ma (stalactite DS-10). Our oldest speleothem age of 1.34 Ma predates the oldest age estimate of the last sea-level highstand at Naracoorte by ~400 ka, based on the AAR age for the East Naracoorte Range of  $938 \pm 178$  ka. These radiometric ages indicate cave initiation at least 0.2–0.5 Ma earlier than previously assumed.

**Charcoal and pollen as indicators of cave opening.** We screened a large pool of dated speleothems (see “Methods”) to produce a set of 66 samples which were analysed for microcharcoal (10–100  $\mu$ m) and pollen concentrations. Pollen and charcoal concentrations (Fig. 4) can be considered independent proxies for cave openness, by which we mean an opening to the surface large enough to allow dynamic airflow (i.e., air speed sufficient to keep dust in suspension) including, but not limited to cave entrances, dolines with entrances and larger solution pipes. Charcoal is likely more reliable because it is much more oxidation-resistant than pollen, and consequently is more frequently observed and more abundant in the NCC speleothems. To use charcoal and pollen in this way, the following taphonomic criteria should be fulfilled: (1) charcoal must be sourced from naturally occurring wildfires on the surface above and not from anthropogenic fires within a cave; (2) drip water must be ruled out as the main mode of transport and (3) the cave must not have experienced significant influx of floodwaters (as it may act as additional sources of charcoal and pollen).

The data reveal a sharp increase in charcoal concentration after ~250 ka. This inflection greatly predates current estimates for earliest human arrival in Australia of around 65 ka<sup>33</sup>, and we do not observe any further increase in charcoal concentrations after

this point. Charcoal concentrations in our speleothem samples are therefore apparently insensitive to any changes in charcoal production and transport related to possible human landscape burning practices over the past ~65 ka. Previous pollen studies<sup>9,34</sup> conclude that drip water is generally not a source of pollen in caves. In our case, we would expect that all speleothems would contain similar charcoal/pollen concentrations if drip water was the dominant source. Instead, a significant portion of the Naracoorte speleothems contain negligible non-calcite residue, in contrast to charcoal-rich samples which typically contain both mineral (e.g., siliciclastic silts, quartz) and biological (e.g., charcoal, pollen, fungal spores, invertebrate remains) dust fractions (Fig. 4 and Supplementary Fig. 2), suggesting that drip water is not an important source of charcoal or pollen within the caves. In addition, a detailed study of karst features and speleogenesis within the NCC<sup>20</sup> suggests that only localised flooding occurred in lower passages after heavy rainfall events. For these reasons, we are confident that the charcoal fragments are primarily wind-derived, and that pollen was transported into the caves either by air currents or by animals (presumably, mainly insects).

Minimum air-flow velocities necessary for the transport of charcoal and pollen into caves have been suggested to vary from 0.01 to 0.1 m/s<sup>35</sup> depending on the particle size (typically 10–100  $\mu$ m). Such velocities generally occur close to cave entrances, or between two entrances when a cave has multiple openings<sup>36</sup>. However, we find charcoal is a common component in speleothems from ventilated caves in multiple Australian cave provinces based on our own unpublished data, suggesting that transport dynamics of microscopic particles into caves may be more complex. Therefore, we interpret higher concentrations of charcoal and pollen in the speleothems as reflecting more dynamic cave ventilation.

In general, we observe an increase in charcoal concentration, and to a lesser extent in pollen concentration, with younger speleothems. The oldest samples (>600 ka) uniformly contain very few charcoal fragments or pollen, indicating that little cave ventilation occurred in the period 1.3 Ma to 600 ka and that, at that time, the caves were most likely closed during speleothem formation. Note that the air flow required to displace the air in a cave is far less than the magnitude required to suspend dusts/aerosols<sup>35</sup>, such as charcoal and pollen within the incoming, lower pCO<sub>2</sub> air. Therefore, large, open cavities are not a prerequisite for speleothem formation as, during the early stages of karst development, CO<sub>2</sub> degassed from seepage waters and/or diffusing through fractures from the overlying soil can be removed via streamflows, small fissures, etc., keeping the pCO<sub>2</sub> low enough for speleothem precipitation.

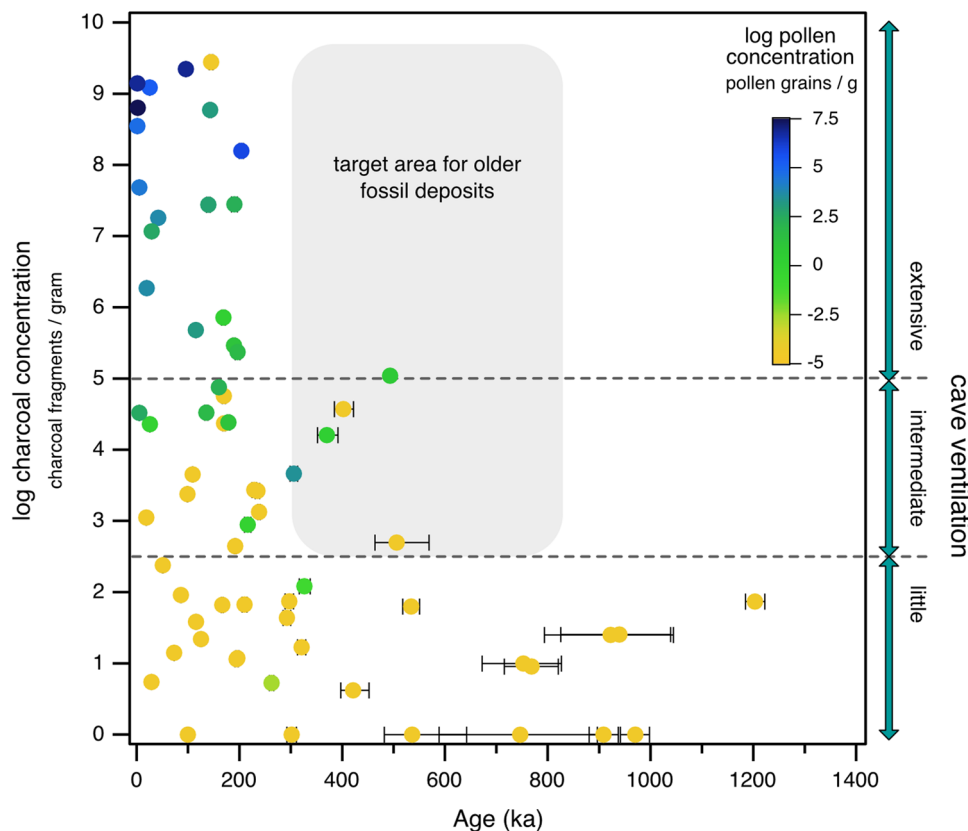


**Fig. 4 Chronology of the Naracoorte Cave Complex in the context of proxies of cave ventilation dynamics.** Charcoal and pollen concentrations within the speleothem samples by age, with  $2\sigma$  uncertainties (whiskers). Charcoal and pollen concentrations are presented on log scales (natural log values  $<2$  indicate  $\leq 7$  pieces of microcharcoal or pollen per gram of calcite) because differences in their abundance between caves, and varying individual speleothem growth rates, are uncontrolled variables. See text for further discussion. Grey box indicates the suggested “sweet spot”: old speleothems with intermediate to high charcoal/pollen contents indicating early cave ventilation, which indicate caves that can serve as potential targets for future studies looking for older vertebrate fossil deposits.

From  $\sim 600$  ka to  $\sim 250$  ka, the pollen content remains low, while more speleothems have charcoal concentrations with intermediate values which we interpret as the initiation of ventilation as caves started to open. A sharp increase in speleothem samples with high charcoal and pollen concentrations is observed from ca. 250 ka, suggesting dynamic airflow through parts of the caves coincident with extensive cave opening. We thus interpret the trend of increasing charcoal concentrations as representing a progressively more open nature of at least seven caves within the NCC (Alexandra, Blanche, Dead Sheep, New, Robertson, Specimen and Victoria Fossil caves) (Supplementary Fig. 3). Another five sites (Bat, Fox, and Whale Bone caves, Henschke and James quarries) are relatively under-sampled for charcoal and pollen but are still consistent with the model developed above in which older speleothems contain fewer charcoal fragments than younger ones. While these caves record high charcoal/pollen concentrations from 250 ka, some passages within each cave must have remained sheltered from dynamic airflow, as we also observe speleothems of all ages with low concentrations. An alternative explanation, that rates of cave ventilation did not change during the past 1 Ma but that biomass burning increased abruptly at  $\sim 250$  ka, is inconsistent with the covariance of charcoal and other mineral and biological dusts.

**Implications for the antiquity of fossil deposits.** Shallow cave systems like the NCC often feature binary modes of sedimentation in which clastic lenses alternate with speleothem deposition<sup>17,37</sup>. At the NCC, solution-pipe cave entrances have

blocked and re-opened over time. Open caves allowed the ingress of sediments, and the accumulation of faunal remains via pitfall entrapment or predator accumulation<sup>17,38,39</sup>. The lack of major sediment reworking provides a well-preserved site stratigraphy and bone deposits. The sharp increase in the number of speleothems with high pollen and charcoal concentrations after 250 ka is consistent with most vertebrate fossil deposits dating to younger than 250 ka. However, while the charcoal and pollen data show that caves were probably largely closed during the oldest phase of speleothem formation (1.3 Ma to 0.6 Ma), the increase in charcoal concentrations after  $\sim 600$  ka shows significant potential for filling the gap in the fossil record beyond 300 ka (Fig. 4).

**Application to cave dynamics.** Speleothems are associated with many of the world’s most diverse Pleistocene vertebrate deposits (e.g. refs. 40–42) and early human remains or artefacts (e.g. refs. 37,43,44). For such settings, the approach we outline here may not only assist with the chronology but also with detecting early signs of cave opening and determining the timing of initiation of palaeo-entrances permitting fossil accumulation. U-Th-Pb dating combined with charcoal/pollen analysis of speleothems allows the detection of cave opening earlier than that suggested by dating the fossil deposits alone and adds a new dimension to understanding the fundamental and dynamic processes of cave evolution. A key finding is that initial cave development started twice as early as initial cave entrance development, which implies that these processes can be widely separated in time. The advantage of our approach is that (1) our use of the U-Th-Pb system provides a

much firmer basis for establishing the minimum age of cave openings than other techniques; and (2) charcoal and pollen are independent proxies which together demonstrate temporal and spatial trends in cave ventilation. Both appear to be powerful indicators of cave ventilation dynamics with implications relevant to many other disciplines concerned with understanding the timing of cave openings. Caves, or sections within them, that contain speleothems with intermediate to high concentrations of charcoal and/or pollen—for example as highlighted in Fig. 4—can then serve as potential targets in the search for older fossil deposits. These techniques can place robust constraints on the temporal extent of the fossil record within any fossil-bearing cave system, of which there are many worldwide.

## Methods

**Cave morphology and speleogenesis at the NCC.** The caves within the NCC are horizontal, phreatic maze systems ranging from small single passages to more complex morphologies with several passages and chambers<sup>20</sup>. The cave entrance types are solution pipes (<1 m diameter and up to 20 m deep) and roof collapse windows (up to 10 m diameter). Currently, several caves have multiple entrances (e.g., Smoke-Tortoise Cave, Blanche Cave, Stick-Tomato Cave and Cathedral Cave), or single entrances (e.g., Whale Bone Cave, Crawford's Dead Sheep Cave, Bat Cave), allowing dynamic air flow through the caves to transport aerosols. The base level of the deepest caves is around  $61 \pm 5$  m ASL<sup>5</sup> and they are located >20 m above the present-day groundwater level.

The East Naracoorte Range (overlying most of the caves, Fig. 1) is the first of a set of Early to Late Pleistocene fossil dunes that record interglacial sea-level high stands westward from Naracoorte to Robe at the present-day coastline. These topographic ridges are preserved parallel to the modern shoreline recording successive sea-level high stands. Chronological studies<sup>18</sup> and references therein showed that the dunes become progressively younger towards the modern shoreline in the southwest. There has been gradual neotectonic uplift in the region during the Pleistocene with the Australian continent slightly tilted north-down, southwest-up<sup>45</sup>. It is generally understood that this uplift was accompanied by progressive relative lowering of the groundwater table and that the caves were never flooded at times of rising sea level<sup>20</sup>, although some aspects of the karst geomorphology require further research.

## Sample collection and preparation, and analytical procedure for U-Th and U-Pb dating.

Samples were collected during three field campaigns from ten caves within the NCC with appropriate sampling permits in all cases. To aid in cave conservation, only previously broken “speleothem rubble” was collected, following the approach of Weij et al.<sup>46</sup>. A range of sample sizes and speleothem types (e.g., flowstones, stalagmites, stalactites, etc.) were used to avoid a sampling bias.

We first dated 74 samples using the U-Th technique, of which 14 were beyond the limit of this chronometer (here taken as those within 3 $\sigma$  of the infinite isochron); these samples were subjected to U-Pb dating. Sampling locations within a given speleothem fragment were constrained by the most suitable regions for dating (i.e., translucent or white calcite)—we did not target a specific zone, such as top or base.

Analytical procedures followed Hellstrom<sup>47</sup> for the U-Th chronology and Woodhead et al.<sup>48</sup> and Engel et al.<sup>49</sup> for the U-Pb chronology. In brief, the U-Th ages were produced from single aliquots (100–200 mg) of individual speleothem rubble samples. These were weighed and dissolved in concentrated nitric acid then spiked and equilibrated using a <sup>229</sup>Th-<sup>233</sup>U-<sup>236</sup>U mixed tracer. U and Th purification used Eichrom ion-exchange columns with a TRU-spec/pre-filter resin-mix followed by sample dry down. After dissolving the purified U-Th samples with a mixed nitric-hydrofluoric acid, they were analysed on a Nu Instruments MC-ICPMS. Two standards, HU-1 and YB-1, with known age were used to test for reproducibility and to correct for instrumental drift. All samples were corrected with a Naracoorte-specific initial <sup>230</sup>Th/<sup>232</sup>Th ratio of  $0.65 \pm 0.35$  using stratigraphic constraint as described in Hellstrom<sup>50</sup>. With the <sup>234</sup>U and <sup>230</sup>Th half-life values of Cheng et al.<sup>30</sup> and Monte-Carlo iterations to solve Eq. (1) in Hellstrom<sup>50</sup>, we calculated corrected ages and their 2 $\sigma$  uncertainty for which the uncertainties of the measured activity ratios as well as the assumed initial <sup>230</sup>Th/<sup>232</sup>Th are fully propagated (Supplementary Data 1 Table 1).

Any ages that exceeded the infinite-age isochron or with an infinite upper bound uncertainty were selected for U-Pb dating (Supplementary Data 1 Table 2). For this, we used five or more aliquots per speleothem sample obtained using a hand-held dental drill. The U-Th and reconnaissance U-Pb analyses revealed that Naracoorte speleothems contain very low U concentrations (between 0.017 and 0.46 ppm, average of 0.092 ppm) and thus very unradiogenic Pb, also of low concentration (between less than 1 ppb and 70 ppb, average of 4.8 ppb). Because of these challenging analytical constraints larger sample aliquots (300–400 mg) were used compared to normal procedures. After obtaining the aliquots, all subsequent steps were performed in a clean-room environment. For U-Pb-elution chemistry, we followed Woodhead et al.<sup>48</sup> and the improved chemical procedure detailed in

Engel et al.<sup>49</sup>. In brief, subsamples were cleaned by repeated washes with a mix of 6 M HCl and ultrapure water. The samples were then dried and weighed, after which they were dissolved completely with 6 M HCl and spiked using a <sup>233</sup>U-<sup>205</sup>Pb tracer. Following Engel et al.<sup>49</sup>, we used a sandwich-resin set-up, meaning that each ion-exchange column was filled with both Eichrom TRU-spec/Pre-filter resin-mix for U purification and extraction and topped with AG1-X8 anion resin for Pb. Once dried, the U and Pb fractions were dissolved in nitric acid and separately measured on a Nu Instruments Plasma MC-ICPMS following Woodhead et al.<sup>48</sup>.

We corrected for instrumental mass bias effects using the sample's internal <sup>238</sup>U/<sup>235</sup>U ratio (137.88) for U and reference material NIST SRM 981 for Pb. Instrument data processing, including mass bias and drift corrections, was performed with an in-house importer within the Iolite environment<sup>51,52</sup>, after which the results were blank-corrected and isotope-dilution calculations were performed.

Where possible, isochrons were constructed using the robust statistical approach of Powell et al.<sup>53</sup>, implemented using the software of Pollard et al.<sup>54</sup>. In cases where the “spine width” was found to exceed the upper 95% confidence limit (indicating that the dataset did not meet the assumptions of this approach), a Model 2 fit<sup>55</sup> was implemented instead.

U-Pb ages were calculated as the intercept point between the isochron and the disequilibrium concordia on a ‘Tera-Wasserburg’ diagram, defined by U-Pb equations equivalent to Ludwig<sup>56</sup> and the inverted <sup>234</sup>U/<sup>238</sup>U age equation<sup>48</sup>, which allows measured <sup>234</sup>U/<sup>238</sup>U values to be incorporated in the numerical solving procedure. The initial <sup>234</sup>U/<sup>238</sup>U activity ratio was calculated using the equation in Woodhead et al.<sup>48</sup>, which is solved iteratively with the <sup>234</sup>U-corrected U-Pb age. Initial activity ratios for other intermediate nuclides <sup>230</sup>Th/<sup>238</sup>U, <sup>226</sup>Ra/<sup>238</sup>U and <sup>231</sup>Pa/<sup>235</sup>U were all assumed equal to 0. Age errors were calculated from 50,000 Monte-Carlo iterations, accounting for full regression fitting errors and analytical errors in the measured <sup>234</sup>U/<sup>238</sup>U activity ratio. Decay constant and natural <sup>235</sup>U/<sup>238</sup>U errors were not included Monte-Carlo simulations, as these sources of error have a negligible impact on such young U-Pb ages. Where minor disagreement exists between U-Th and U-Pb age determinations of the same samples, U-Pb ages are preferred due to the greater susceptibility of very old U-Th ages to low levels of post-depositional U mobility.

## Sample preparation and analytical procedure for charcoal and pollen analyses.

To evaluate the extent of cave opening and cave ventilation during speleothem deposition, we extracted fossil pollen and charcoal from the speleothem samples using analytical procedures adapted from Sniderman et al.<sup>57,58</sup> and Matley et al.<sup>59</sup>. We screened a large pool of dated samples by their visual appearance (silty textures, opaque, laminated and/or dark-coloured calcite, rather than translucent and/or white calcite) and by their <sup>230</sup>Th/<sup>232</sup>Th ratio, to produce a set of 66 samples, which were analysed for microcharcoal (10–100  $\mu$ m in size) and pollen concentrations (Supplementary Table 2 and Supplementary Data 1 Table 3).

In brief, for all speleothems analysed, a reconnaissance aliquot of ca. 15 g was taken. These were weighed, washed repeatedly in distilled water, then etched with 1 M HCl for 5–10 min to remove possible modern contaminant pollen. Samples were then rinsed repeatedly in distilled water and spiked with one tablet containing a known number of *Lycopodium* spores (available from Lund University, Sweden) in order to permit later estimation of pollen and charcoal concentrations. Samples were then dissolved in concentrated HCl, and the residues rinsed with distilled water, centrifuged and decanted, after which the residues were treated for 24 h with cold, concentrated HF, then diluted with 1 M HCl, centrifuged and rinsed with distilled water. Samples with voluminous, organic-rich residues were then acetolysed in a 9:1 mixture of acetic anhydride and concentrated sulfuric acid at 90 °C for 8 min. Finally, samples were dehydrated in ethanol, and mounted in glycerol on glass slides. Pollen and charcoal were counted at  $\times 320$  and  $\times 640$  magnifications on a Zeiss Axiolab A1 compound microscope fitted with N-Achroplan objectives. Charcoal was defined as all angular, opaque objects >10  $\mu$ m in diameter. Pollen percentage data will be presented in a subsequent publication.

**Potential biases.** To avoid a sampling bias, we randomly collected speleothem rubble samples throughout the caves with respect to distance from the cave entrance. We did not record the spatial distribution of our samples: some rubble samples were in situ, evidenced by intact parts of stalagmites and stalactites on cave floors and roofs but many other samples were clearly transported small distances, most likely by the cave management when preparing for visitor paths in show caves. More importantly, our conclusions are unaffected by whether the rubble samples are in situ or transported within a cave.

The age difference between top and base of individual stalagmites is small on average (Supplementary Table 3), and so any “sample position bias” is unlikely to influence our results significantly over the timescale of the dataset.

The aliquots targeted for charcoal and pollen analysis were mostly taken from the same section as the aliquot for U-Th dating, but not always. The pollen/charcoal aliquots had to be an order of magnitude larger than the U-Th aliquots in order to extract a statistically significant amount of charcoal fragments and pollen. In this paper, the point is that there is a major increase in charcoal density after ca 250 ka. For that pattern to be an artefact of mismatches between sample U-Th age

and the age of the sample's charcoal/pollen aliquot, the mismatch would need to be at least tens of kyr, probably more (rather than single-digit kyr differences, which are possible). We top-bottom dated several stalagmites from a larger pool of NCC samples (not all included in this study) to understand the typical lifespan of a speleothem (Supplementary Table 3 and Supplementary Fig. 4). The results show that NCC stalagmites are relatively short-lived, i.e., not longer than ~27 ka on average. Most charcoal/pollen aliquots were sampled within the age uncertainty of the U-Th aliquot, and, on the timescale of the entire dataset, any age discrepancy between U-Th and pollen/charcoal aliquots will not change the conclusions of this paper.

We believe climate/ecosystem changes are not the primary cause of the changes in charcoal/pollen concentrations at NCC over the past ~1 Ma. This is because, first, if our pollen and charcoal concentration records were primarily responses to vegetation change, then the low pollen and charcoal concentrations in most samples prior to ca. 250 ka would imply a landscape containing essentially no vegetation, or a situation in which all pollen has been destroyed by oxidation, and in which no wildfire occurred, over ca. 1 Ma. This is inconsistent with Neogene and Quaternary vegetation records in southern Australia (e.g. refs. 57,58), which are dominated by fire-dependent vegetation and taxa. Therefore, the more parsimonious explanation for the observed increase in charcoal and pollen concentrations is that, prior to ca. 250 ka, most speleothems were protected from bio- and mineral-dust by the lack of cave openings. We are confident that the distance from any modern cave entrance does not bias our data, because we sampled randomly throughout the caves and most samples will reside close to their point of origin, and yet still see a clear transition in charcoal and pollen concentrations at ca. 250 ka.

## Data availability

The datasets generated during the current study are available at <https://doi.org/10.25375/uct.20495136>. Additionally, all isotope data needed to reproduce the U-Th and U-Pb ages and U-Pb isochrons are also available in Supplementary Data 1 Tables 1 and 2, and all data used to generate Figs. 1 and 4 are also available in Supplementary Tables 1 and 2 and Supplementary Data 1 Table 3.

Received: 29 March 2022; Accepted: 22 August 2022;

Published online: 26 September 2022

## References

- Stock, G. M., Granger, D. E., Sasowsky, I. D., Anderson, R. S. & Finkel, R. C. Comparison of U-Th, paleomagnetism, and cosmogenic burial methods for dating caves: implications for landscape evolution studies. *Earth Planet. Sci. Lett.* **236**, 388–403 (2005).
- Häuselmann, P., Plan, L., Pointner, P. & Fiebig, M. Cosmogenic nuclide dating of cave sediments in the Eastern Alps and implications for erosion rates. *Int. J. Speleol.* **49**, 3 (2020).
- Harmon, R., Thompson, P., Schwarcz, H. & Ford, D. Uranium-series dating of speleothems. *Natl. Speleol. Soc. Bull.* **37**, 21–33 (1975).
- Richards, D. A., Bottrell, S. H., Cliff, R. A., Ströhle, K. & Rowe, P. J. U-Pb dating of a speleothem of Quaternary age. *Geochim. Cosmochim. Acta* **62**, 3683–3688 (1998).
- Woodhead, J. D. et al. The antiquity of Nullarbor speleothems and implications for karst palaeoclimate archives. *Sci. Rep.* **9**, 1–8 (2019).
- Scott, A. C. Charcoal recognition, taphonomy and uses in palaeoenvironmental analysis. *Palaeogeogr. Palaeoclimatol. Palaeoecol.* **291**, 11–39 (2010).
- Gradziński, M., Hercman, H., Nowak, M. & Bella, P. Age of black coloured laminae within speleothems from Domica Cave and its significance for dating of prehistoric human settlement. *Geochronometria* **28**, 39–45 (2007).
- Desmarchelier, J., Hellstrom, J. & Spate, A. Constraining relative wildfire frequency in the Australian alps over the past 500,000 years, using U-Th dating of speleothem-encapsulated soot layers. In *Biennial Conference of the Australasian Quaternary Association, Cradle Mountain, Tasmania*. (2004).
- McGarry, S. F. & Caseldine, C. Speleothem palynology: an undervalued tool in Quaternary studies. *Quat. Sci. Rev.* **23**, 2389–2404 (2004).
- Coles, G., Gilbertson, D., Hunt, C. & Jenkinson, R. Taphonomy and the palynology of cave deposits. *Cave Sci.* **16**, 83–89 (1989).
- Reed, E. H. & Bourne, S. J. Pleistocene fossil vertebrate sites of the south east region of South Australia II. *Trans. R. Soc. S. Aust.* **133**, 30–40 (2009).
- Atkins, R. A., Hill, R. S., Hill, K. E., Munroe, S. E. & Reed, E. H. Preservation quality of plant macrofossils through a Quaternary cave sediment sequence at Naracoorte, South Australia: Implications for vegetation reconstruction. *Rev. Palaeobot. Palynol.* **299**, 104607 (2022).
- Prideaux, G. J. et al. Mammalian responses to Pleistocene climate change in southeastern Australia. *Geology* **35**, 33–36 (2007).
- Roberts, R. G. et al. New ages for the last Australian megafauna: continent-wide extinction about 46,000 years ago. *Science* **292**, 1888–1892 (2001).
- Priya et al. ESR and OSL dating of fossil-bearing deposits from Naracoorte Cave Complex palaeontological sites, south Australia. *Quat. Geochronol.* **69**, 101270 (2022).
- Arnold, L. et al. Examining sediment infill dynamics at Naracoorte cave megafauna sites using multiple luminescence dating signals. *Quat. Geochronol.* **70**, 101301 (2022).
- Moriarty, K. C., McCulloch, M. T., Wells, R. T. & McDowell, M. C. Mid-Pleistocene cave fills, megafaunal remains and climate change at Naracoorte, South Australia: towards a predictive model using U-Th dating of speleothems. *Palaeogeogr. Palaeoclimatol. Palaeoecol.* **159**, 113–143 (2000).
- Murray-Wallace, C. V. *Quaternary History of the Coorong Coastal Plain, Southern Australia* (Springer International Publishing, 2018).
- Sandiford, M. Neotectonics of southeastern Australia: linking the Quaternary faulting record with seismicity and in situ stress. *Geol. Soc. Aust. Spec. Publ.* **22**, 101–113 (2003).
- White, S. & Webb, J. A. The influence of tectonics on flank margin cave formation on a passive continental margin: Naracoorte, Southeastern Australia. *Geomorphology* **229**, 58–72 (2015).
- Idnurm, M. & Cook, P. J. Palaeomagnetism of beach ridges in South Australia and the Milankovitch theory of ice ages. *Nature* **286**, 699–702 (1980).
- Huntley, D., Hutton, J. & Prescott, J. The stranded beach-dune sequence of south-east South Australia: a test of thermoluminescence dating, 0–800 ka. *Quat. Sci. Rev.* **12**, 1–20 (1993a).
- Huntley, D., Hutton, J. & Prescott, J. Further thermoluminescence dates from the dune sequence in the southeast of South Australia. *Quat. Sci. Rev.* **13**, 201–207 (1994a).
- Huntley, D. & Prescott, J. R. Improved methodology and new thermoluminescence ages for the dune sequence in south-east South Australia. *Quat. Sci. Rev.* **20**, 687–699 (2001).
- Huntley, D., Lian, O., Hu, J. & Prescott, J. Tests of luminescence dating making use of paleomagnetic reversals. *Ancient TL* **12**, 28–30 (1994b).
- Banerjee, D. et al. New quartz SAR-OSL ages from the stranded beach dune sequence in south-east South Australia. *Quat. Sci. Rev.* **22**, 1019–1025 (2003).
- Murray-Wallace, C. V., Brooke, B., Cann, J., Belperio, A. & Bourman, R. Whole-rock aminostratigraphy of the Coorong Coastal Plain, South Australia: towards a 1 million year record of sea-level highstands. *J. Geol. Soc.* **158**, 111–124 (2001).
- Fuchs, M. & Owen, L. A. Luminescence dating of glacial and associated sediments: review, recommendations and future directions. *Boreas* **37**, 636–659 (2008).
- Miller, G. H., Kaufman, D. & Clarke, S. Amino acid dating. *Encyclopedia of Quaternary Science: Second Edition*, (eds Elias, S. E. & Mock, C. J.), 37–48 (Elsevier Inc., 2013).
- Cheng, H. et al. Improvements in <sup>230</sup>Th dating, <sup>230</sup>Th and <sup>234</sup>U half-life values, and U-Th isotopic measurements by multi-collector inductively coupled plasma mass spectrometry. *Earth Planet. Sci. Lett.* **371**, 82–91 (2013).
- Ayliffe, L. K. et al. 500 ka precipitation record from southeastern Australia: evidence for interglacial relative aridity. *Geology* **26**, 147–150 (1998).
- Ayliffe, L. & Veeh, H. Uranium-series dating of speleothems and bones from Victoria Cave, Naracoorte, South Australia. *Chem. Geol. Isot. Geosci. Sect.* **72**, 211–234 (1988).
- Clarkson, C. et al. Human occupation of northern Australia by 65,000 years ago. *Nature* **547**, 306–310 (2017).
- Burney, D. A. & Burney, L. P. Modern pollen deposition in cave sites: experimental results from New York State. *New Phytol.* **124**, 523–535 (1993).
- Dredge, J. et al. Cave aerosols: distribution and contribution to speleothem geochemistry. *Quat. Sci. Rev.* **63**, 23–41 (2013).
- Gradziński, M., Gorny, A., Pazdur, A. & Pazdur, M. F. Origin of black coloured laminae in speleothems from the Kraków-Wieluń; Upland, Poland. *Boreas* **32**, 532–542 (2003).
- Pickering, R. et al. Stratigraphy, U-Th chronology, and palaeoenvironments at Gladysvale Cave: insights into the climatic control of South African hominin-bearing cave deposits. *J. Hum. Evol.* **53**, 602–619 (2007).
- Reed, E. World Heritage values and conservation status of the Australian Fossil Mammal Sites (Riversleigh/Naracoorte). *Z. für Geomorphol.* **62**, 213–233 (2021).
- Reed, E. H. Pinning down the pitfall: entry points for Pleistocene vertebrate remains and sediments in the Fossil Chamber, Victoria Fossil Cave, Naracoorte, South Australia. *Quat. Australas.* **25**, 2–8 (2008).
- Jass, C. N. & George, C. O. An assessment of the contribution of fossil cave deposits to the Quaternary paleontological record. *Quat. Int.* **217**, 105–116 (2010).
- Prideaux, G. J. et al. Timing and dynamics of Pleistocene mammal extinctions in southwestern Australia. *Proc. Natl. Acad. Sci. USA* **107**, 22157–22162 (2010).

42. Barnosky, A. D. et al. Exceptional record of mid-Pleistocene vertebrates helps differentiate climatic from anthropogenic ecosystem perturbations. *Proc. Natl. Acad. Sci. USA* **101**, 9297–9302 (2004).
43. Jaubert, J. et al. Early Neanderthal constructions deep in Bruniquel Cave in southwestern France. *Nature* **534**, 111–114 (2016).
44. Hoffmann, D. L., Angelucci, D. E., Villaverde, V., Zapata, J. & Zilhão, J. Symbolic use of marine shells and mineral pigments by Iberian Neandertals 115,000 years ago. *Sci. Adv.* **4**, eaar5255 (2018).
45. Sandiford, M. The tilting continent: a new constraint on the dynamic topographic field from Australia. *Earth Planet. Sci. Lett.* **261**, 152–163 (2007).
46. Weij, R., Woodhead, J., Hellstrom, J. & Sniderman, K. An exploration of the utility of speleothem age distributions for palaeoclimate assessment. *Quat. Geochronol.* **60**, 101112 (2020).
47. Hellstrom, J. Rapid and accurate U/Th dating using parallel ion-counting multi-collector ICP-MS. *J. Anal. At. Spectrom.* **18**, 1346–1351 (2003).
48. Woodhead, J. et al. U–Pb geochronology of speleothems by MC-ICPMS. *Quat. Geochronol.* **1**, 208–221 (2006).
49. Engel, J., Maas, R., Woodhead, J., Timpel, J. & Greig, A. A single-column extraction chemistry for isotope dilution U–Pb dating of carbonate. *Chem. Geol.* **531**, 119311 (2020b).
50. Hellstrom, J. U. –Th dating of speleothems with high initial <sup>230</sup>Th using stratigraphical constraint. *Quat. Geochronol.* **1**, 289–295 (2006).
51. Paton, C., Hellstrom, J., Paul, B., Woodhead, J. & Hergt, J. Iolite: Freeware for the visualisation and processing of mass spectrometric data. *J. Anal. At. Spectrom.* **26**, 2508–2518 (2011).
52. Paul, B. et al. CellSpace: a module for creating spatially registered laser ablation images within the Iolite freeware environment. *J. Anal. At. Spectrom.* **27**, 700–706 (2012).
53. Powell, R., Green, E. C., Marillo Sialer, E. & Woodhead, J. Robust isochron calculation. *Geochronology* **2**, 325–342 (2020).
54. Pollard, T. J., Woodhead, J., Engel, J., Hellstrom, J. & Drysdale, R. DQPB: Software for calculating disequilibrium U–Pb ages. *Geochronology* (under review).
55. Ludwig, K. Isoplot/Ex rev. 2.49: a geochronological tool kit for Microsoft Excel. Berkeley Geochronology Center 55 (2001).
56. Ludwig, K. R. Effect of initial radioactive-daughter disequilibrium on U–Pb isotope apparent ages of young minerals. *J. Res. US Geol. Surv* **5**, 663–667 (1977).
57. Sniderman, J. K. et al. Pliocene reversal of late Neogene aridification. *Proc. Natl. Acad. Sci. USA* **113**, 1999–2004 (2016).
58. Sniderman, J. et al. Vegetation and climate change in southwestern Australia during the Last Glacial Maximum. *Geophys. Res. Lett.* **46**, 1709–1720 (2019b).
59. Matley, K. A., Sniderman, J. K., Drinnan, A. N. & Hellstrom, J. C. Late-Holocene environmental change on the Nullarbor Plain, southwest Australia, based on speleothem pollen records. *Holocene* **30**, 672–681 (2020).
60. Grealy, A. et al. An assessment of ancient DNA preservation in Holocene–Pleistocene fossil bone excavated from the world heritage Naracoorte Caves, South Australia. *J. Quat. Sci.* **31**, 33–45 (2016).
61. Macken, A., McDowell, M., Bartholomeusz, D. & Reed, E. Chronology and stratigraphy of the Wet Cave vertebrate fossil deposit, Naracoorte, and relationship to paleoclimatic conditions of the Last Glacial Cycle in south-eastern Australia. *Aust. J. Earth Sci.* **60**, 271–281 (2013a).
62. Darrenougue, N. et al. A late Pleistocene record of aeolian sedimentation in Blanche Cave, Naracoorte, South Australia. *Quat. Sci. Rev.* **28**, 2600–2615 (2009).
63. St Pierre, E., Zhao, J.-x & Reed, E. Expanding the utility of Uranium-series dating of speleothems for archaeological and palaeontological applications. *J. Archaeol. Sci.* **36**, 1416–1423 (2009).
64. St Pierre, E., Zhao, J.-x, Feng, Y.-x & Reed, E. U-series dating of soda straw stalactites from excavated deposits: method development and application to Blanche Cave, Naracoorte, South Australia. *J. Archaeol. Sci.* **39**, 922–930 (2012).
65. Macken, A. C. et al. Application of sedimentary and chronological analyses to refine the depositional context of a Late Pleistocene vertebrate deposit, Naracoorte, South Australia. *Quat. Sci. Rev.* **30**, 2690–2702 (2011).
66. Grün, R., Moriarty, K. & Wells, R. Electron spin resonance dating of the fossil deposits in the Naracoorte Caves, South Australia. *J. Quat. Sci.* **16**, 49–59 (2001).
67. Brown, S. P. & Wells, R. T. A middle Pleistocene vertebrate fossil assemblage from cathedral cave, Naracoorte, South Australia. *Trans. R. Soc. S. Aust.* **124**, 91–104 (2000).

### Acknowledgements

We acknowledge that we worked on the lands of the First Nations Peoples who have been the Custodians for thousands of years and we acknowledge and pay our respects to their Elders past and present. We thank the Naracoorte Caves management team for providing access to the caves on the park as well as the owners of caves on private properties. We also thank our Naracoorte research partners Terre à Terre Pty Ltd, Department of Environment and Water, Naracoorte Lucindale Council, Wrattonbully Wine Industries Association Inc, South Australian Museum, and Defence Science and Technology Group. Thanks also to Petra Bajo, John Engel, Serene Paul, Roland Maas for laboratory and data processing assistance. R.W. thanks Robyn Pickering for her support. We thank Patrick Moss, Sylvia Reichelmann and one anonymous reviewer for their comments and suggestions. This work was facilitated by Australian Research Council grants FL160100028 to J.D.W., FT130100801 to J.C.H., LP160101249 to E.R., R.N.D. and J.C.H. and a Postgraduate Writing-Up Award supported by the Albert Shimmins Fund to R.W.

### Author contributions

R.W., J.D.W., J.M.K.S. and E.R. conceived and designed the study. R.W. wrote the manuscript and created the figures, with contributions from the other authors. R.W., J.D.W., E.R., R.N.D. and S.B. conducted the fieldwork. R.W. and J.C.H. performed and/or contributed to the U–Th analysis and post-processing. R.W., J.D.W. and T.J.P. performed and/or contributed to the U–Pb analysis and post-processing. J.M.K.S. performed the charcoal and pollen analyses. All authors contributed comments and/or revisions to the manuscript.

### Competing interests

The authors declare no competing interests.

### Additional information

**Supplementary information** The online version contains supplementary material available at <https://doi.org/10.1038/s43247-022-00538-y>.

**Correspondence** and requests for materials should be addressed to Rieneke Weij.

**Peer review information** *Communications Earth & Environment* thanks Patrick Moss, Sylvia Reichelmann and the other, anonymous, reviewer(s) for their contribution to the peer review of this work. Primary Handling Editor: Joe Aslin.

**Reprints and permission information** is available at <http://www.nature.com/reprints>

**Publisher's note** Springer Nature remains neutral with regard to jurisdictional claims in published maps and institutional affiliations.



**Open Access** This article is licensed under a Creative Commons Attribution 4.0 International License, which permits use, sharing, adaptation, distribution and reproduction in any medium or format, as long as you give appropriate credit to the original author(s) and the source, provide a link to the Creative Commons license, and indicate if changes were made. The images or other third party material in this article are included in the article's Creative Commons license, unless indicated otherwise in a credit line to the material. If material is not included in the article's Creative Commons license and your intended use is not permitted by statutory regulation or exceeds the permitted use, you will need to obtain permission directly from the copyright holder. To view a copy of this license, visit <http://creativecommons.org/licenses/by/4.0/>.

© The Author(s) 2022